Title

The Design, Construction, and Operation of a Differential Micromanometer Part I. Electronics

Author

Lamers, Kenneth W

Publication Date

1964-10-01

UCRL-11218, Pt. I

University of California

Ernest O. Lawrence Radiation Laboratory

THE DESIGN, CONSTRUCTION, AND OPERATION OF A DIFFERENTIAL MICROMANOMETER

PART I. ELECTRONICS

Research and Development

UCRL-11218, Pt. I

UC-37 Instruments
TID-4500 (34th Ed.)

UNIVERSITY OF CALIFORNIA

Lawrence Radiation Laboratory
Berkeley, California

AEC Contract No. W-7405-eng-48

THE DESIGN, CONSTRUCTION, AND OPERATION OF A DIFFERENTIAL MICROMANOMETER

PART I. ELECTRONICS

Kenneth W. Lamers

October 16, 1964

Printed in USA. Price $2.00. Available from the Clearinghouse for Federal Scientific and Technical Information, National Bureau of Standards, U. S. Department of Commerce, Springfield, Virginia.

THE DESIGN, CONSTRUCTION, AND OPERATION OF A DIFFERENTIAL MICROMANOMETER

PART I. ELECTRONICS

Contents

THE DESIGN, CONSTRUCTION, AND OPERATION OF A DIFFERENTIAL MICROMANOMETER

PART I. ELECTRONICS

Kenneth W. Lamers

Lawrence Radiation Laboratory
University of California
Berkeley, California

October 16, 1964

ABSTRACT

Part I of this report covers the electronics of a micromanometer designed to measure pressure differentials on the order of 0.1 micron with an accuracy of 3%. The micromanometer is to be used in conjunction with a Wrede gauge, a device that converts atomic concentration into a pressure differential. The pressure difference is sensed by a membrane manometer constructed in the form of a differential capacitor that forms two legs of a resonant-bridge network excited by a radio-frequency source. The bridge output (2.7 mc) is amplified and fed to a phase-sensitive detector that determines the direction of unbalance and develops a dc voltage that restores the membrane essentially to its initial position. The restoring voltage is directly proportional to pressure differential and is indicated by a recorder.

Micromanometers of this type are not new. What this report describes that has not been described before are: (1) details of frequency considerations; and (2) selection of parameters that lead to increased bridge sensitivity.

Electrical performance only is described in Part I of this report. Total performance and theory are described in Part II.

I. INTRODUCTION

We are interested in measuring very small atomic concentrations. A number of techniques are available, but only one principal type is considered here, that in which atomic concentration is converted into a pressure differential.

Differential-pressure devices are attractive for this measurement because they are responsive to the intrinsic property of the quantity to be measured. In particular, we hope to measure pressure differentials on the order of 0.1 μ with an accuracy of 3%. These pressures are very minute and are in a region difficult to measure. Instrumentation with such capabilities can facilitate the measurement of other pressure phenomena--those that cannot now be measured with the necessary precision.

The principal advantage of mechanical pressure sensors over other types of sensors is that the mechanical ones yield a measurement independent of the nature of the gas. For other methods in which electrical or thermal properties are used, a calibration (or at least a correction) is necessary for each gas and the methods are not applicable for every gas.

Membrane manometers have been developed for measuring very low pressures. If they are used in conjunction with an electronic system employing negative feedback, it is possible to obtain a calibration that is both linear and independent of membrane properties. Several such systems are described in the literature. We chose to pattern ours after one described by Opstelten, Warmoltz, and van Zelst.[1]

Another technique for measuring very small atomic concentrations involves thermal instrumentation, which is generally simpler than differential-pressure instrumentation. With this thermal technique, the heat of recombination of atoms on a surface is sensed and converted into a temperature difference. The thermal sensing elements, however, perturb the system and are less discriminating against phenomena not of interest. Thus we do not consider thermal types, but limit our discussion to pressure-differential types.

II. GENERAL CONSIDERATIONS

Our primary objective is to develop the simplest possible instrument, one that can be constructed and operated by those with little or no electronic background. As several units are required for the experiment planned, simplicity is paramount. Furthermore, an instrument that is readily duplicated can be a useful tool to other experimenters.

Assuming that simplicity was the prime consideration, we chose to hold electronic circuitry to a minimum. The most practical approach, as discussed in other articles,[2] seems to be that of a resonant bridge such as is shown in Fig. 1. The resonance condition, by exaggerating capacitive changes at the membrane, reduces complexity of the associated circuitry.

The circuit of Fig. 1 has other virtues. Bridge symmetry, for example, reduces sensitivity to frequency changes and to changes in coil resistance, R. Also important, the low output impedance of the bridge permits us to locate the manometer remotely without concern for the capacity due to

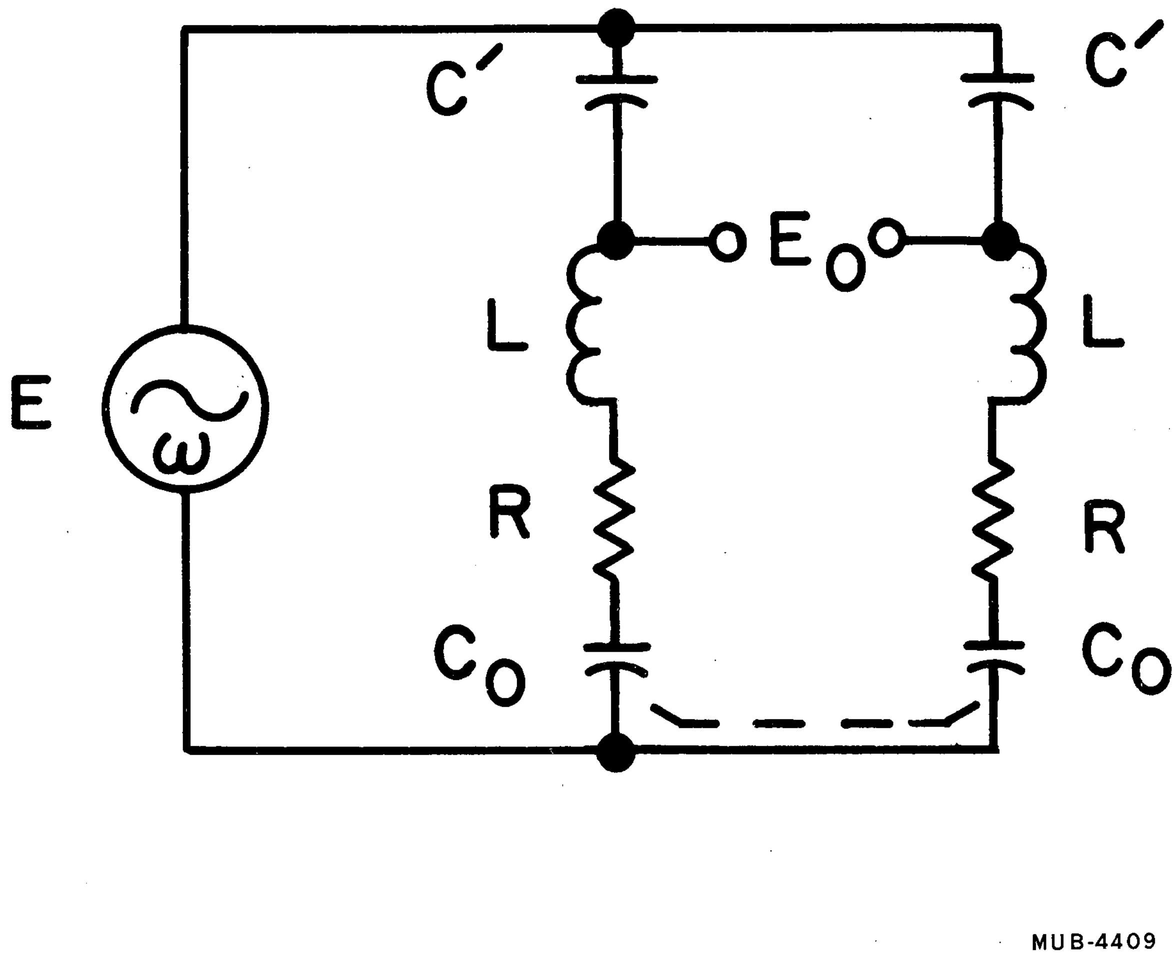

Fig. 1. Resonant-bridge network. Here E is the bridge excitation voltage, E_0 is the bridge output voltage, C_0 is the manometer capacitance in each leg, R is the ac resistance of L, and $LC_0 = 1/\omega^2$, with $\omega = 2\pi f$ where f is the frequency.

connecting cables. The remote feature is useful because the manometer can be enclosed by a separate chamber where the temperature is held to close tolerances. This is especially important when one considers the extremely small capacitance changes resulting from the pressure differentials to be recorded. To a first estimate, we expect capacitance changes on the order of one part in 10^4 for a pressure differential of 0.1 micron. The actual change is related to the properties of the manometer developed, but it is quite apparent that temperature control is necessary.

With regard to the bridge, we expressed the condition of resonance, and so turn our attention to frequency. Most relevant articles devote little time to frequency considerations, and so we decided to explore that facet more thoroughly. With this in mind, we derived an expression relating sensitivity to frequency and the pertinent bridge parameters. The results of that derivation can be expressed[3]

$$S = 2\left(\frac{\delta C_0}{C_0}\right)\frac{1}{\left(R^2 + \frac{1}{\omega^2 C'^2}\right)\omega^2 C_0 C'} \qquad (1)$$

where S represents bridge sensitivity; i.e., the ratio of output to input voltage E_0/E resulting from a given unbalance, $\delta C_0/C_0$. The remaining symbols correspond to the parameters shown in Fig. 1.

Sensitivity, however, is not the only consideration. In practice, we wish to make the output voltage independent of small changes in frequency and coil resistance. This is true if $1/\omega^2 C'^2$ is considerably greater than R^2, and Eq. (1) reduces to

$$S \approx 2\,(C'/C_0)\,(\delta C_0/C_0). \qquad (2)$$

Substituting for sensitivity, bridge output for a given unbalance becomes

$$E_0 \approx 2E\,(C'/C_0)\,(\delta C_0/C_0), \qquad (3)$$

and we find that the bridge output, E_0, is essentially insensitive to small changes in frequency and coil resistance.

Equation (2) shows that bridge sensitivity is directly proportional to C'/C_0 when $1/\omega^2 C'^2$ is considerably greater than R^2. When satisfying stability requirements, therefore, we find that sensitivity becomes independent of frequency. This is fortuitous in the sense that it permits us to choose a frequency that is convenient without sacrificing sensitivity.

With regard to C'/C_0, Eq. (2) would seem to indicate that we should make that ratio as high as possible. This is true except for modifying influences, one of which is the distributed capacity shunting the coils of Fig. 1. Elaborating, we desire series resonance wherein the reactances of L and C_0 are equal but opposite. When a fixed frequency is assumed, a decrease in C_0 demands increased inductance, L, in order to satisfy the resonance condition. Higher inductance values, however, have more distributed capacity, and so we end up with a coil self resonant to a frequency that has been considerably lowered. If the inductance is increased enough its self-resonant frequency falls below the excitation frequency, and so the coil acts capacitive. This reduces bridge sensitivity because the LC legs are no longer series resonant.

The trick, then, is to choose a value of C_0 that is considerably greater than the distributed capacitance of the coil chosen for the bridge. This insures that L appears inductive rather than capacitive, and permits us to realize the desired series resonance for L and C_0.

In our case, we chose to work backwards from a particular coil, deducing an acceptable value of C_0. In particular, we selected National Radio coil form XR50, one wound with 64 turns of #32 Formvar. The selection was based upon practical considerations such as: (a) availability (b) physical size and construction (c) distributed capacity (d) coil quality factor (Q) (e) adaptability to transformer construction if used in the null detector, and (f) adjustable inductance.

With regard to frequency, the fore-mentioned coil self resonates to approximately 25 mc with the slug at the center position. With the assumption that the bridge is excited with one-tenth that frequency to minimize the self-resonance effect described, the bridge would be excited with something like 2.5 mc. As a number of surplus crystals were available at 2.765 mc, we decided to operate at the latter frequency.

A simple calculation reveals that when the slug is near the center position (L is about 40 μH), series-resonance is achieved when C_0 is approximately 75 pF.

Concerning C', its reactance must be considerably greater than R, the ac resistance of L (about 6 ohms), if bridge output is to be independent of small changes in frequency and coil resistance. Stability requirements, then, indicate that C' should be small. Sensitivity, on the other hand, is increased if we make C' larger. The upper limit is dictated by the source impedance that drives the bridge. If, for example, C' is exorbitant, bridge input impedance relative to that of the source is very low, and so only a small fraction of the generator voltage is available at the bridge input terminals.

In view of the foregoing considerations, we chose to make C' 250 pF, a value compatible with each of the conditions listed. In clarification, C' represents a reactance of 230 ohms. This is considerably greater than the 6 ohms associated with R, and it is a reasonable ratio for satisfying the stability requirements relative to Eq. (2). The ratio is considerably less than that of Opstelten[1] (2700-Ω reactance for C_0 and 15 ohms for R), but this is countered somewhat by use of a crystal-controlled oscillator.

Bridge sensitivity depends upon the ratio C'/C_0. Our ratio is 250/75, as compared to 120/250 for Opstelten,[1] and so the sensitivity obtained with our design would appear to be approximately 7 times greater than that obtained with their design.

With regard to generator impedance, the buffer-plate resistance is about 3000 ohms. The generator drives the circuit shown on Fig. 2, one that transforms bridge input impedance to 4400 ohms. This matching increases bridge excitation voltage, compensating for the low reactance of C' (230 ohms).

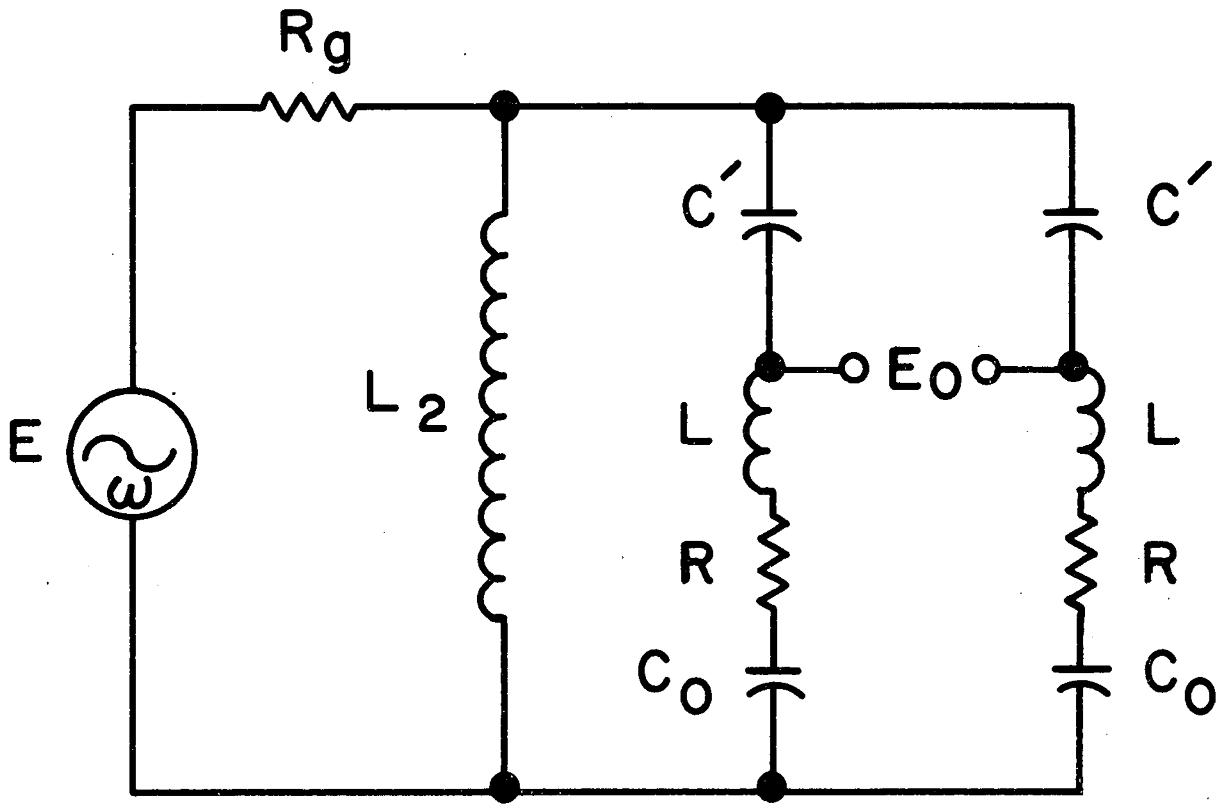

Fig. 2. Resonant bridge with matching network. Here R_g is the generator impedance and $L_2C' = 1/2\omega^2$. Other parameters are defined in the legend of Fig. 1.

III. CIRCUIT DESCRIPTION

The electrical system comprises four basic units as shown in the block diagram, Fig. 3. These are:

1. Generator – Fig. 4
2. Transducer element – Fig. 5
3. Null detector – Fig. 6
4. Power supply – Fig. 7

Physical construction is illustrated by the photographs of Figs. 8 through 15.

A. Generator

This is a crystal-controlled oscillator plus buffer. The crystal is operated series resonant with feedback determined by the ratio of capacitors C1 and C2. The divider ratio and bias are adjusted to produce a minimum of distortion. The divider also reduces oscillator loading, improving frequency stability.

Buffer excitation is low to prevent V2 from drawing grid current. The coupling capacitor and bias are adjusted for purity of waveform. The low plate resistance (3000 ohms) of V2 permits us to increase the value of C' and improve sensitivity.

A differential capacitor, C_g, compensates for inequalities of the bridge and simplifies balancing.

B. Transducer Element

This element includes a membrane manometer fashioned in the form of a differential capacitor. The capacity of each side is the same, about 75 pF. This unit also includes two coils for resonating each half of the transducer to the excitation frequency. When tuned to resonance, each leg presents a low impedance, approximately 6 ohms, to the generator.

C. Null Detector

The null detector comprises two amplifiers and a phase-sensitive detector. Both amplifiers, signal and reference, are tuned to the generator frequency of 2.765 mc. The signal-amplifier gain is approximately 10^5, the reference-amplifier gain about 50. Both amplifiers are designed around miniature Nuvistor-type tetrodes. High transconductance combined with low interelectrode capacitance permit considerable gain without neutralization.

The phase detector is a synchronous rectifier employing two diodes. Both diodes are gated in phase by a common reference voltage (2.765 mc from the generator), and conduct during the same half cycle. When the bridge is unbalanced, a signal component is added in series with the reference voltage applied to each diode. This signal component is in phase with the reference at one diode, out of phase at the other. The signal and reference are in phase at only one diode — which one depending upon the direction of bridge unbalance. The reference and signal voltages have the same frequency because they are derived from a common source, the generator.

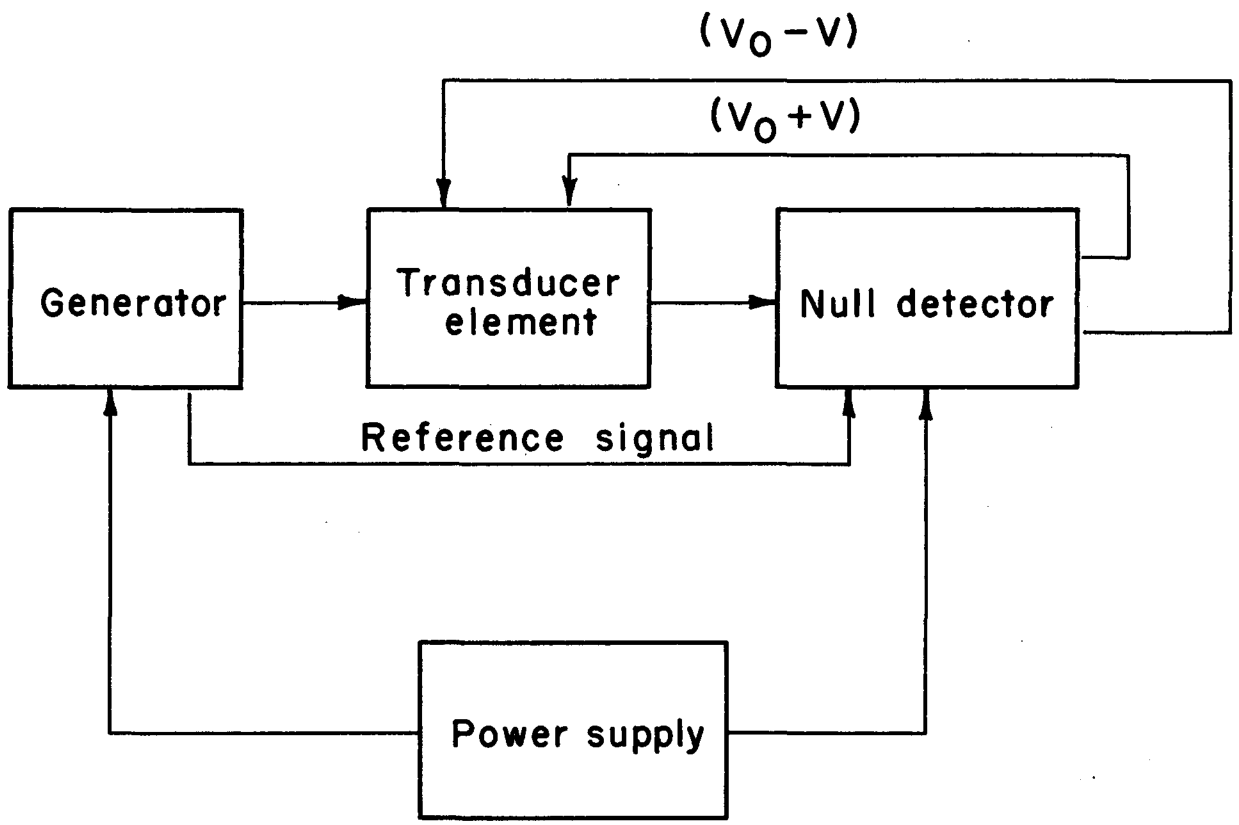

Fig. 3. Block diagram of the electrical system. Here $V_0 + v$ is the restoring voltage applied to one plate, and $V_0 - v$ is the restoring voltage applied to the other.

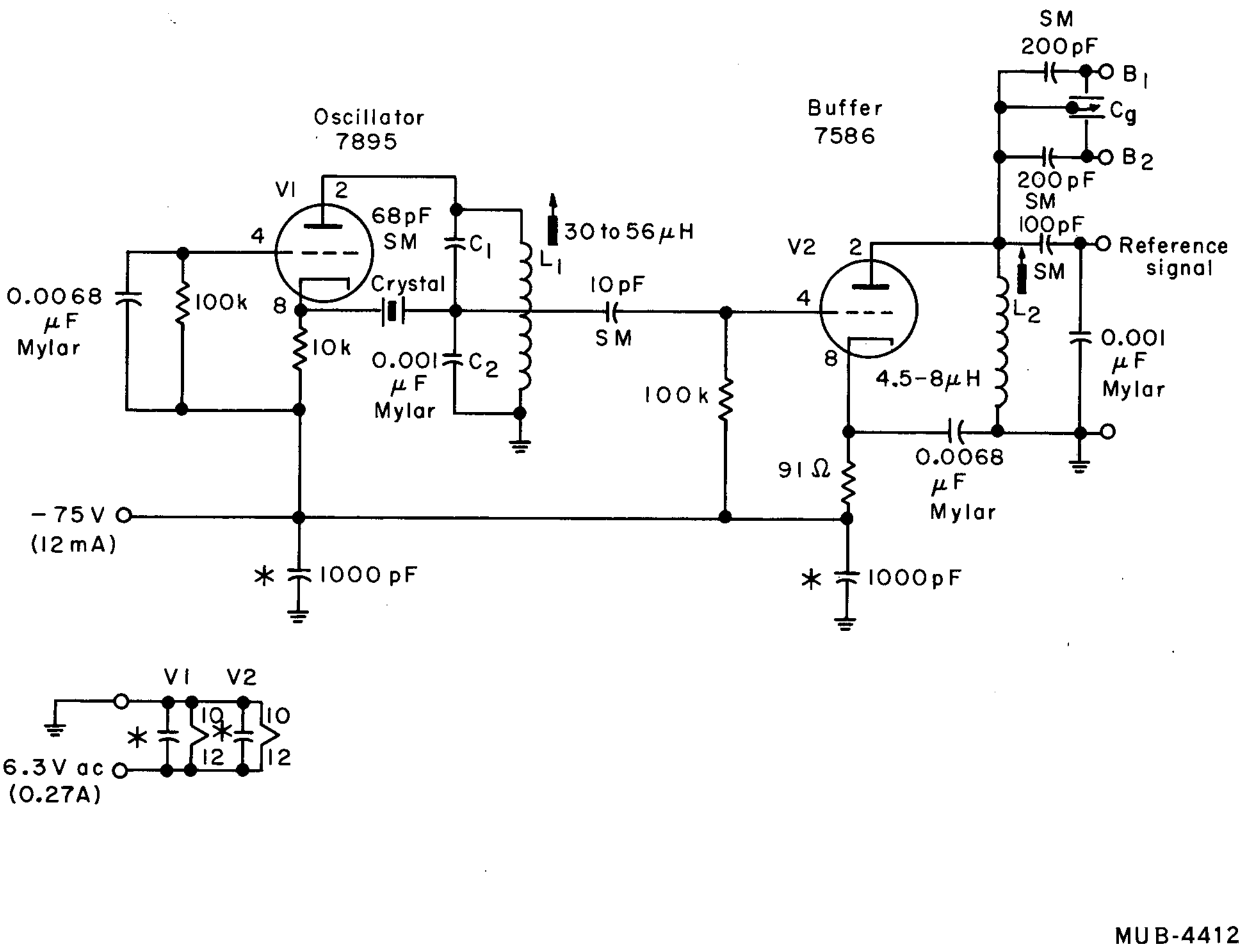

Fig. 4. Schematic diagram of the generator. All resistors are 1/4 W. Inductance L_1 comprises 64 turns of No. 32 Formvar wound on National Radio Corp. form XR50; L_2 is 25 turns of No. 22 Formvar wound on form XR50. The crystal (type CR-18/U) operates at 2762.500 kc/sec. C_g is a 4.5- to 100-pF differential variable air capacitor, type S, No. 148-306 manufactured by E. F. Johnson Co. Capacitors marked with an asterisk are 1000-pF ceramic feed-through type; those indicated by SM are silver-mica. Tubes V1 and V2 are Nuvistors.

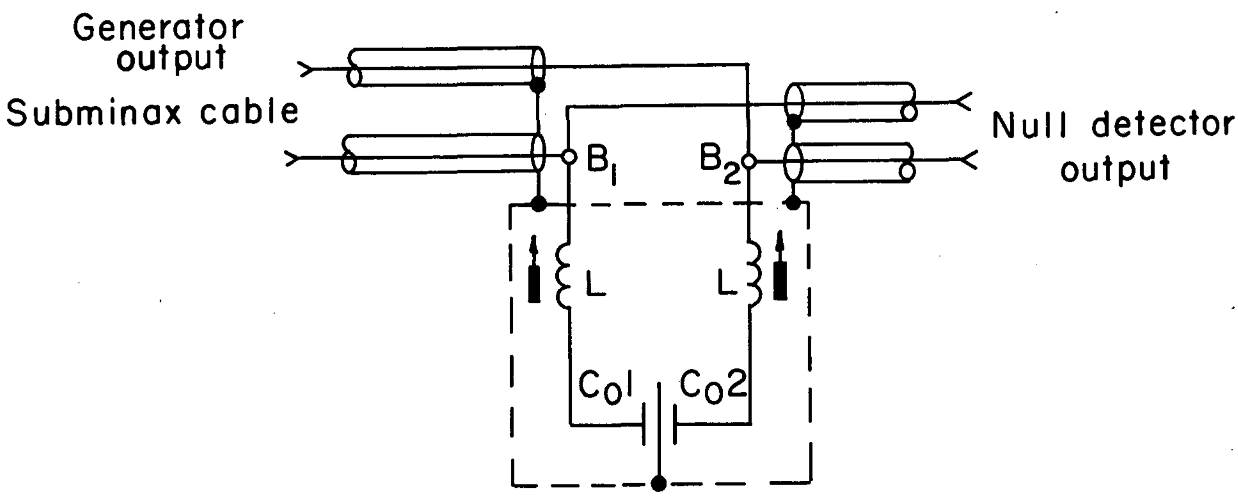

MUB-4413

Fig. 5. Transducer element (within dashed lines). Terminals B_1 and B_2 connect to corresponding terminals of both the generator and the null detector. Capacitances $C_0 1$ and $C_0 2$ of each side of the membrane manometer are about 75 pF. Inductance L is 64 turns of No. 32 Formvar wound on National Radio Corp. form XR50.

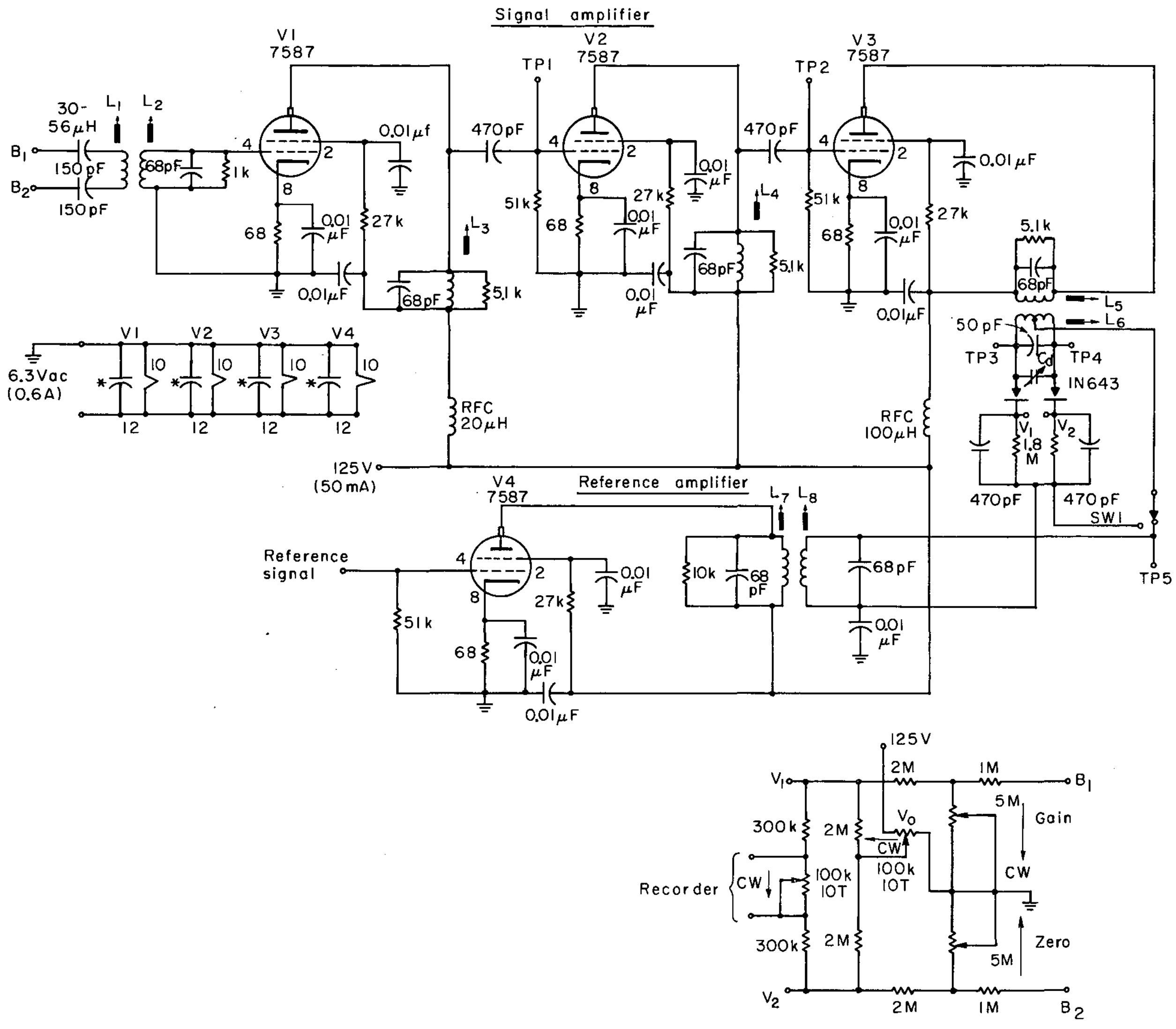

MUB-4415

Fig. 6. Schematic diagram of the null detector. The 27k resistors are 1/2 W; all others are 1/4 W. Asterisks denote 1000-pF ceramic feed-through capacitors, C_d is a 4- to 30-pF ceramic trimmer, all other pF capacitors are silver-mica, and all μF capacitors are Mylar. The 7587 is an RCA Nuvistor. Coils L_1 through L_8 comprise 64 turns of No. 32 Formvar wound on National Radio Corp. form XR50; L_6 is center-tapped. All coils are wound counterclockwise viewed from the tuning end. Inductances L_1 and L_2, L_5 and L_6, L_7 and L_8 are mounted as shown in Figs. 8 and 13 to form transformers.

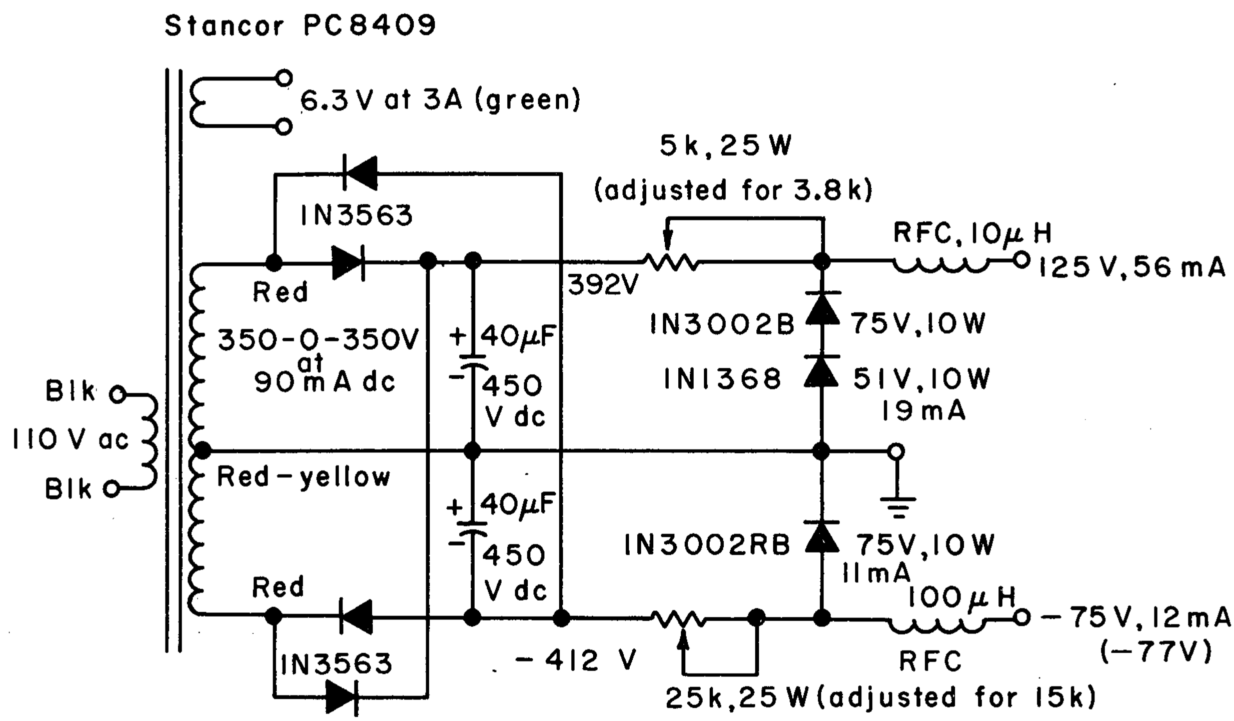

MUB-4414

Fig. 7. The power supply. All voltages and currents were measured when operating with a Sola voltage-regulating transformer. Without this transformer, 392V becomes 453V, -412V becomes -486V, 19 mA becomes 32 mA, and 11 mA becomes 15.4 mA. The 40-μF capacitors should have a 500-V working voltage if the Sola transformer is not used.

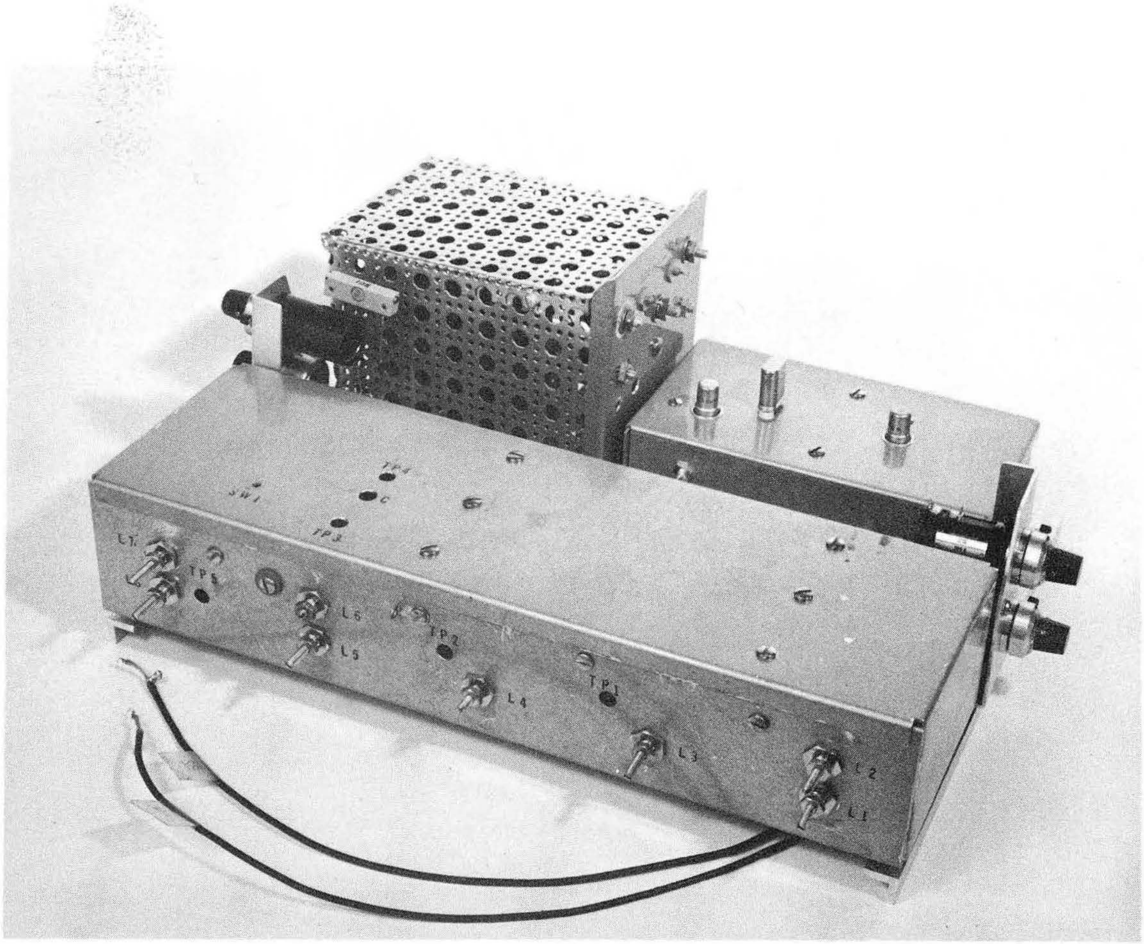

ZN-4548

Fig. 8. Top-front view of the electronics. The remotely located pressure transducer is not shown. Construction is modular. The null detector is in the foreground. The power supply is at left rear; the generator module is to its right.

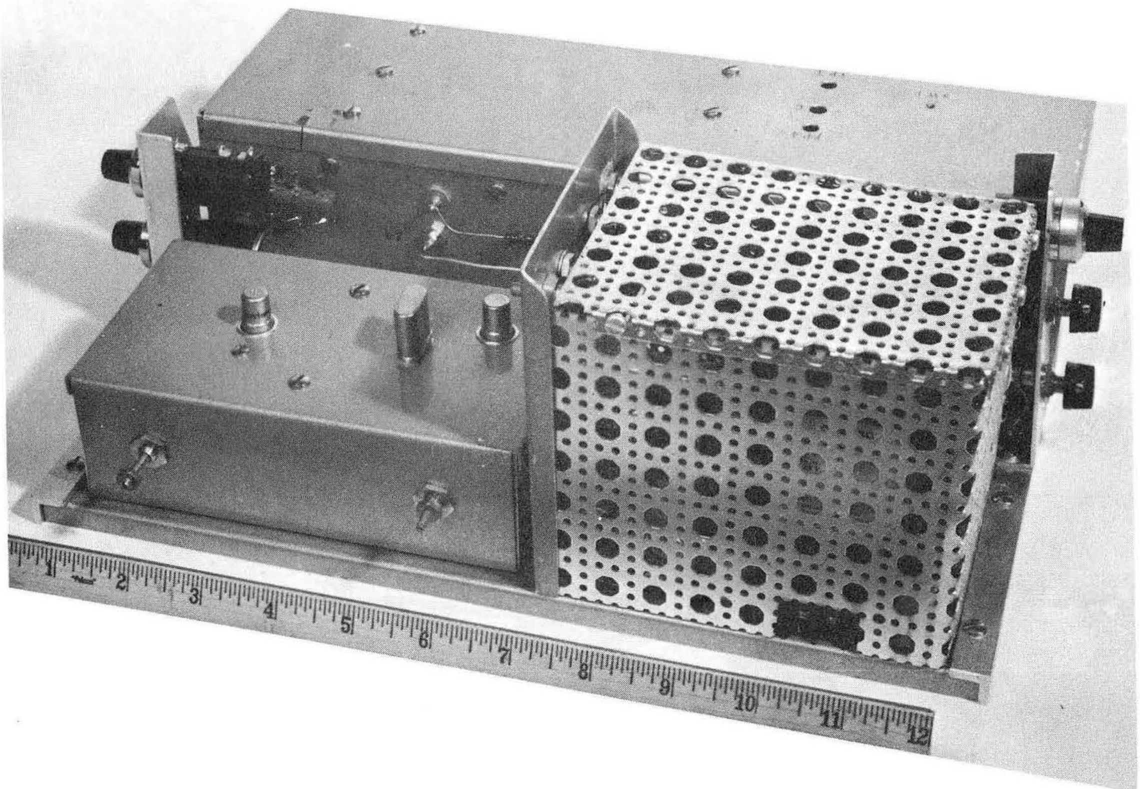

ZN-4549

Fig. 9. Top rear view of the electronics. The generator module at left includes two Nuvistor-type tubes and a crystal, all mounted on the top of the module. Slugs tuning L_1 and L_2 are at right and left, respectively. Power supply, covered by calcaine shield, is at right-front. Controls at the right, top to bottom, are recorder, gain, and zero. Controls at the left were added subsequent to writing the text and may prove unnecessary.

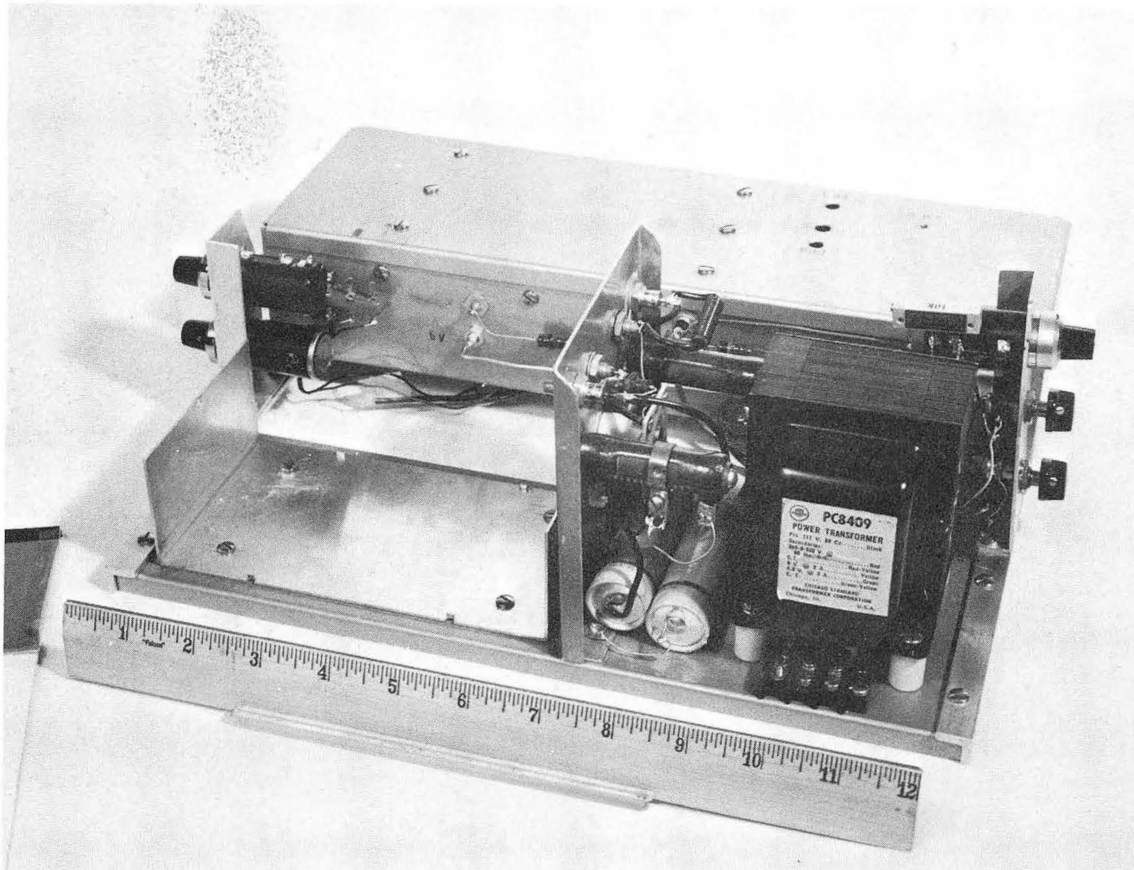

ZN-4550

Fig. 10. Power supply, with calcaine cover removed. The generator module, normally mounted left front, has been removed to indicate the manner of mounting. Angle brackets unitizing the modules can be seen to the left and right. The power supply and generator modules are mounted on a plate formed from a cover identical to the one shown on the null detector.

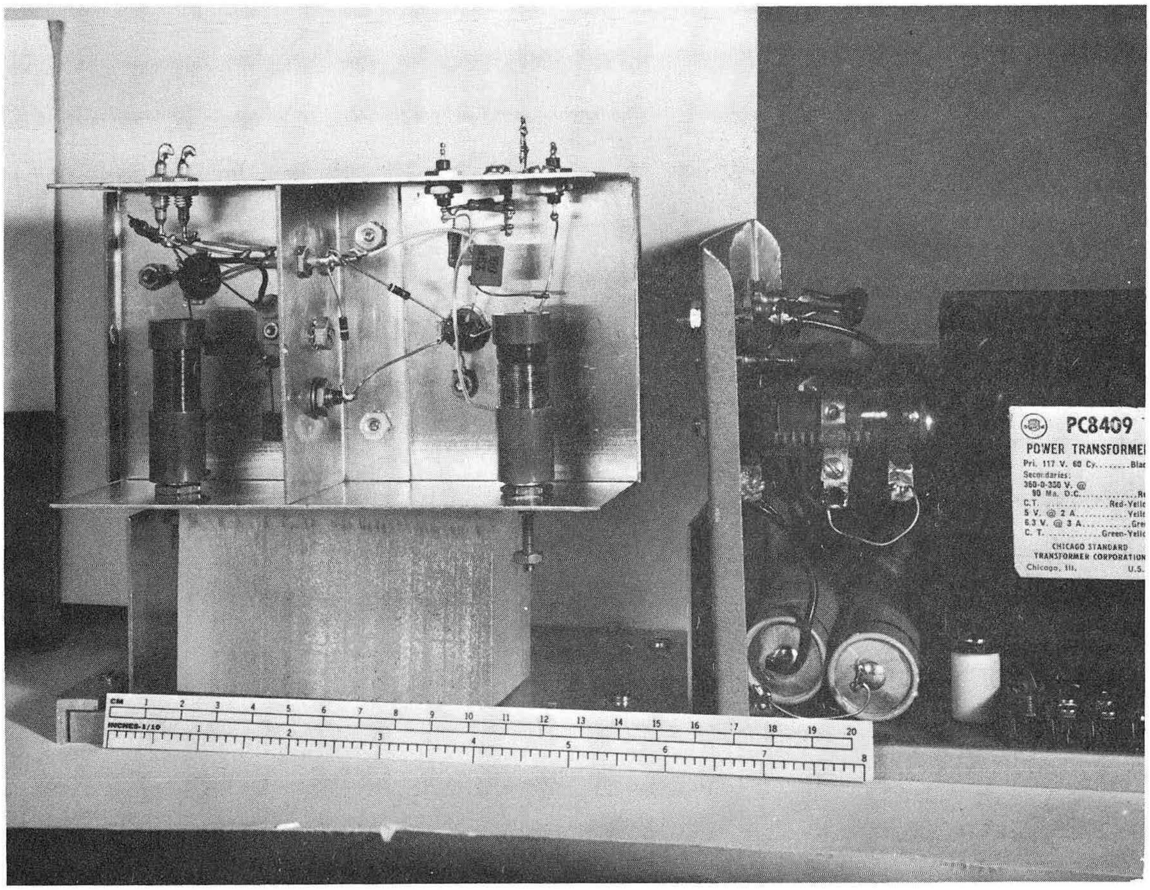

ZN-4551

Fig. 11. Generator module tilted so that it can be viewed from underneath. The oscillator compartment is to the left, buffer at right.

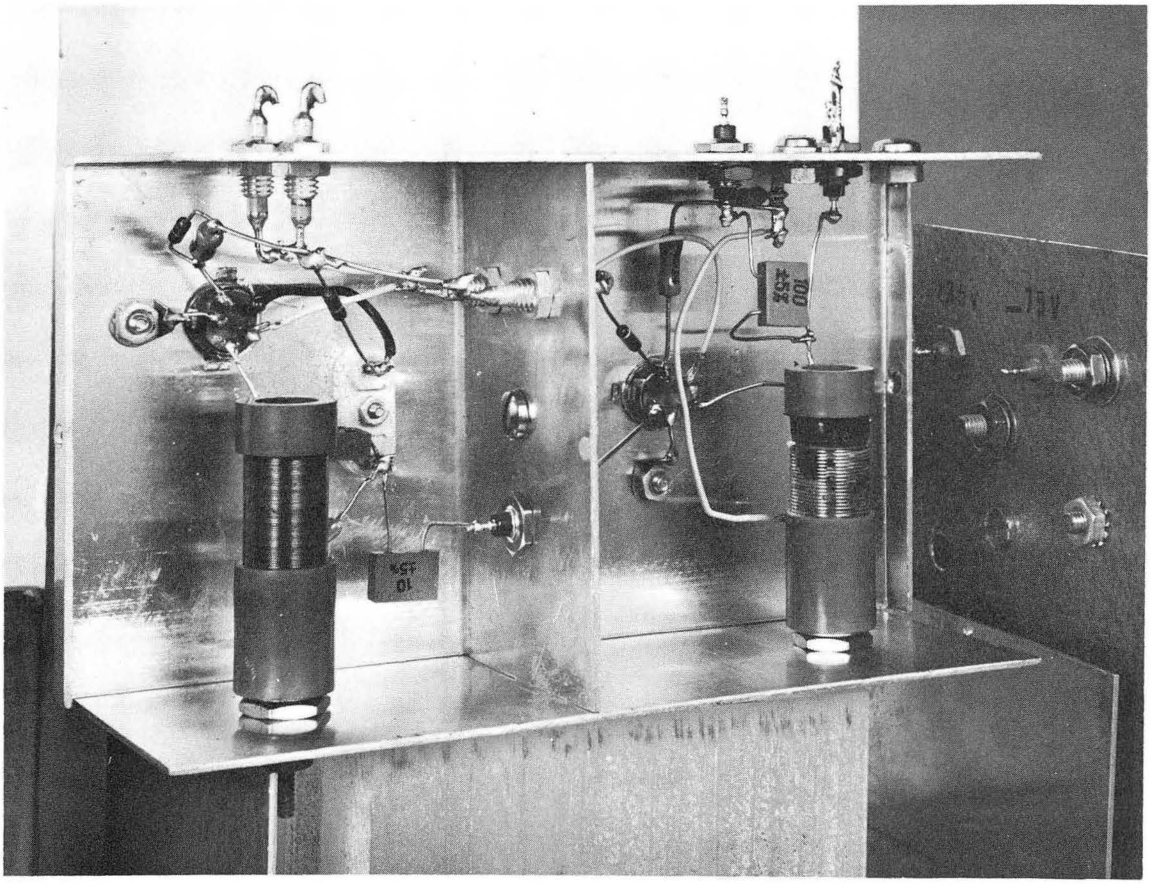

ZN-4552

Fig. 12. Expanded view of the generator module, showing construction in detail.

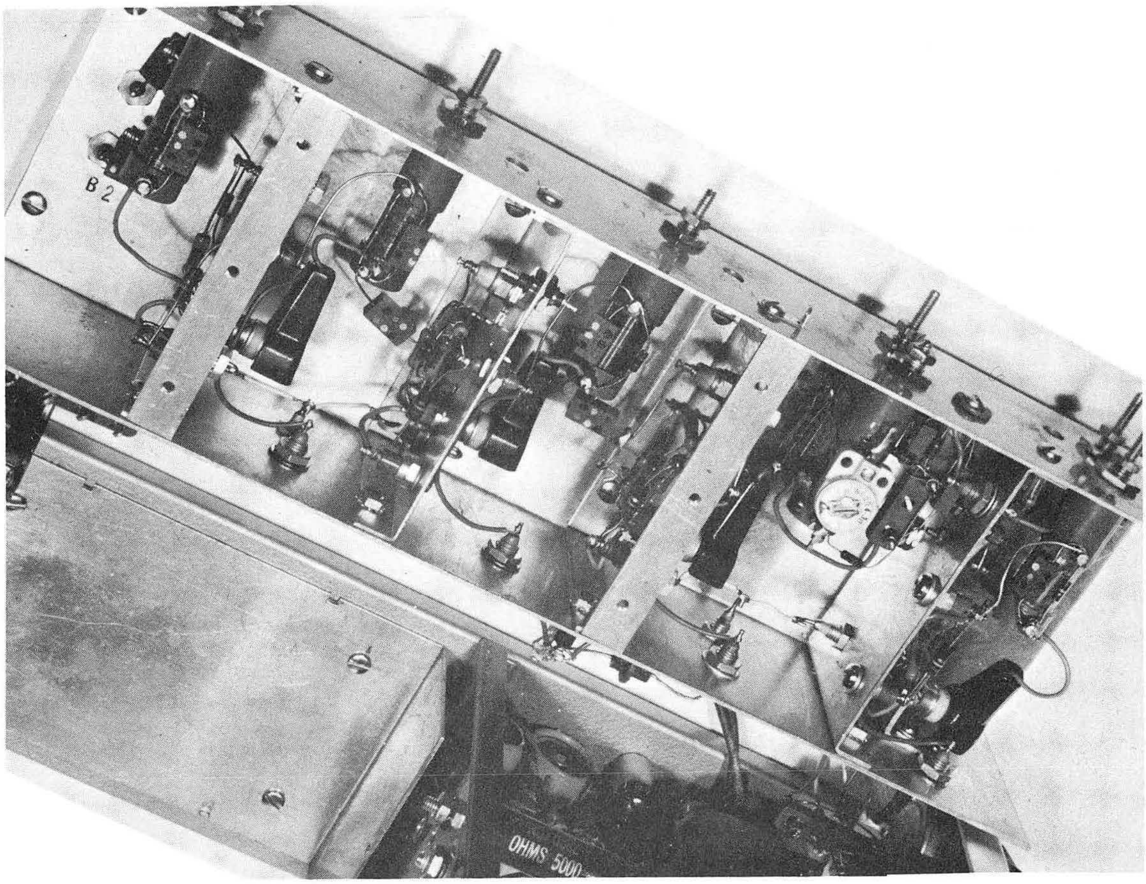

ZN-4553

Fig. 13. Null detector, top-front view with cover removed. The unit is separated into compartments. It is important that two of the dividing plates (second from left and the one at the right) be tapped to receive screws holding the top cover-plate down. This tapping improves intercompartment shielding, and helps to prevent oscillation.

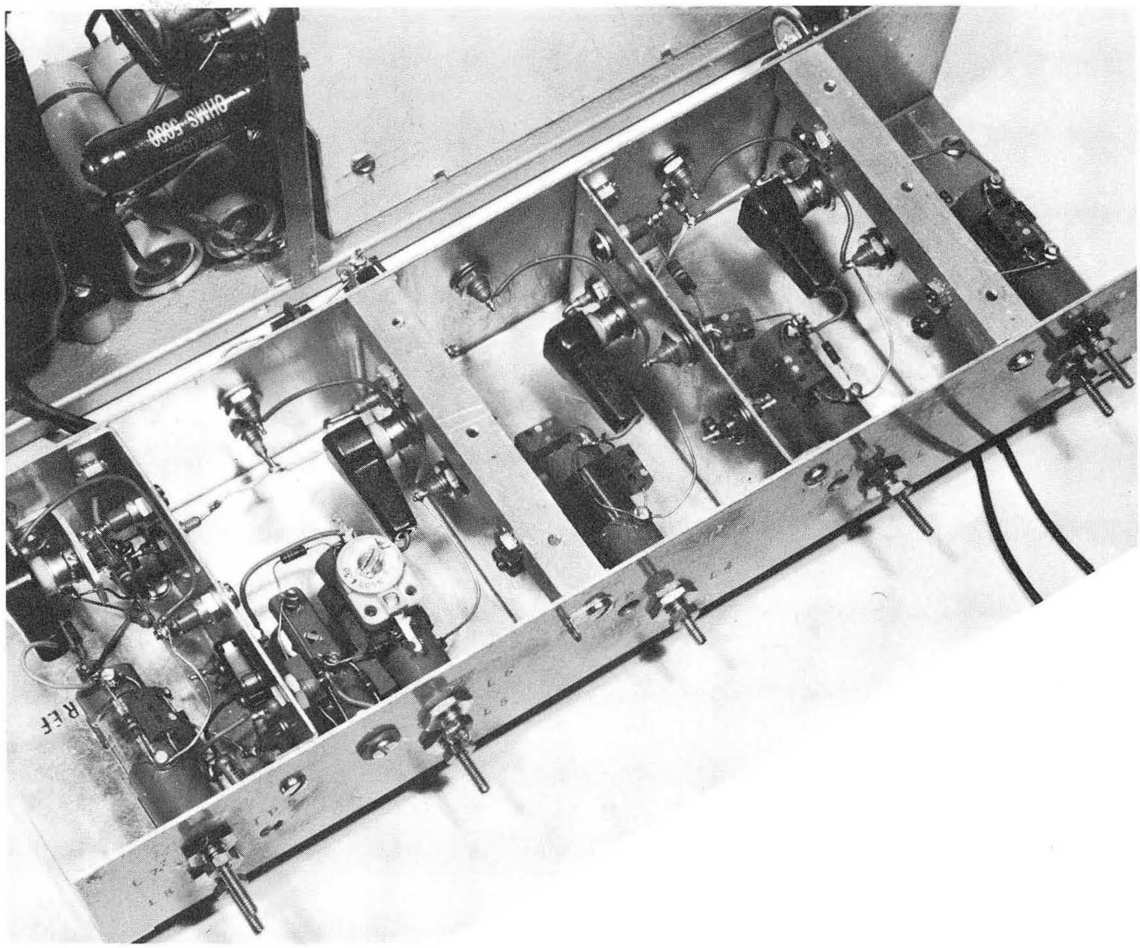

ZN-4554

Fig. 14. Top left view of null detector, illustrating construction in detail.

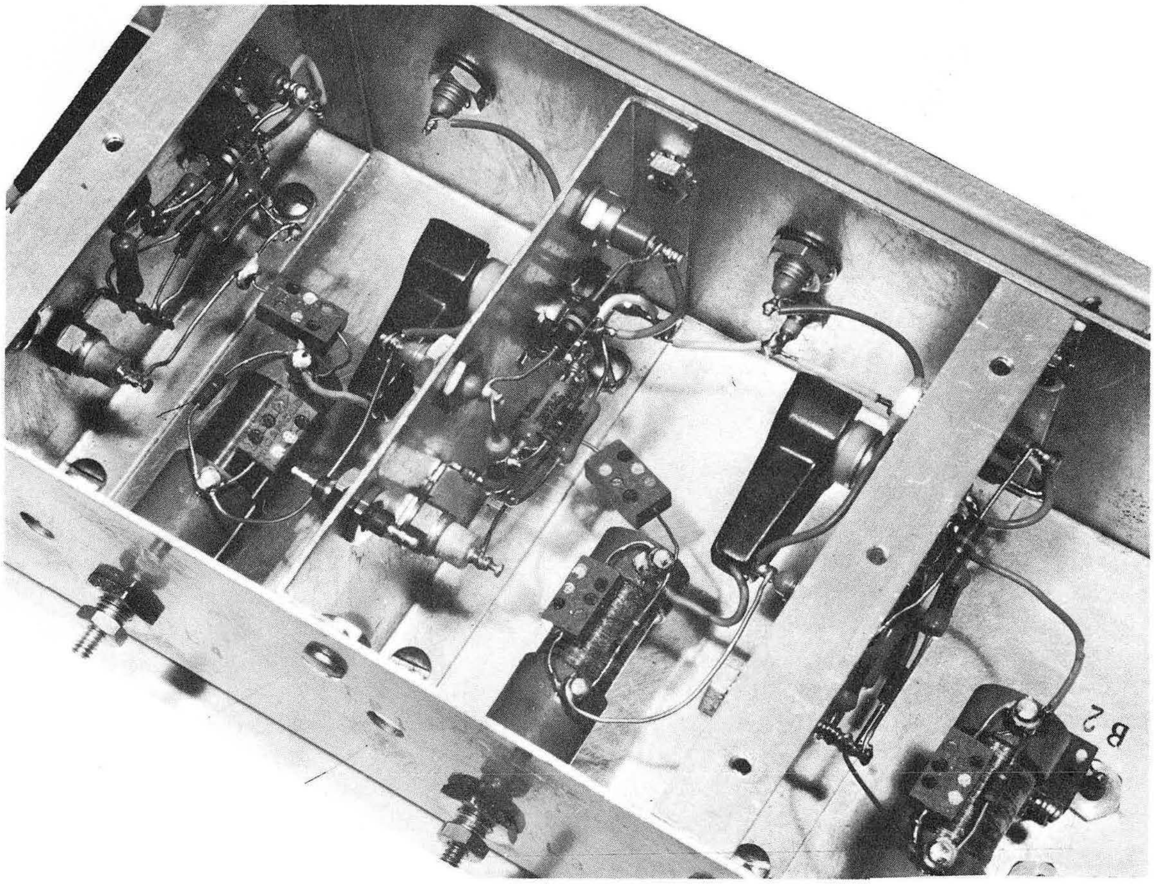

ZN-4555

Fig. 15. Inner compartments of the null detector viewed from above and right.

At any rate, detector output is a dc voltage, the polarity of which depends upon the direction of bridge unbalance. The magnitude of that voltage is proportional to the degree of unbalance. Detector-output voltage is applied to the manometer with a phasing that restores the membrane to essentially its initial position (position of zero pressure difference). The restoring voltage required is directly proportional to differential pressure, and it is this voltage that is recorded.

D. Power Supply

The power supply is conventional, zener diodes regulating to the voltages required. A negative supply permits the diaphragm to be grounded directly, eliminating the need for shunt feed to the buffer tube V2 of the generator. The positive supply furnishes the reference voltage V_0.

IV. PERFORMANCE

It is difficult to evaluate total performance because a satisfactory manometer is not yet available. The manometer tested is an experimental version and is extremely temperature sensitive. This temperature sensitivity stems from its construction, which is highly adjustable to facilitate evaluation of the requirements imposed upon the electronics system proper. It was particularly useful in determining gain requirements, but the very qualities that lend to its versatility tend to make it temperature sensitive. Cursory tests indicated that the capacity of each side of the diaphragm varied from 75 pF at 28°C to about 95 pF at 20°C. The direction of change indicates that its Plexiglas construction is probably responsible. This is substantiated by two effects: (a) The capacity decreases with temperature, and (b) both sides change in the same direction. If we assume that a temperature control of 0.1°C or better can be achieved, the variation in capacity might be reduced to one part per thousand. Furthermore, if the opposing plates were suspended differently and with another material, we might achieve stabilities approaching 1 ppm.

Frequency stability has not yet been evaluated. Gain, voltage and current, coil, and transformer measurements are presented in the appendix.

V. TUNING PROCEDURE

A. Generator

These instructions can be followed by reference to Fig. 4.

1. Set the differential capacitor C_g to its center (half capacity) position.
2. Connect terminals B_1 and B_2 to ground.
3. Monitor Ref jack with an oscilloscope probe (oscilloscope frequency response should be at least 3mc), and tune L1 and L2 for maximum. We normally operate about 0.8 volt, peak to peak (pp), with a 7-pF probe and with all other cables disconnected from the Ref jack.
4. Remove the short, terminals B_1 and B_2, to ground.

B. Transducer Element

Note: Before making the following adjustments, set the loop gain, V_0, and zero controls to their counterclockwise positions (Fig. 6). For the rest of the instructions given in B, consult Fig. 5.

1. Monitor B_1 with scope probe; tune C_01 for minimum (C_01 and C_02 were adjustable in the experimental manometer).

2. Monitor B_2 with scope probe; tune C_02 for minimum.

3. If a dual-trace oscilloscope is available, set to "alternate sweep" and monitor B_1 and B_2 with separate probes. Superimpose the waveforms, then adjust C_01, C_02, and C_g (generator) until the waveforms are identical in shape and amplitude.

4. Steps 1, 2, and 3 are the coarse adjustment for null. A fine adjustment is made by connecting a scope probe to monitor TP1 at the null detector (Fig. 6), then adjusting C_01 and C_g (generator) for minimum. If greater sensitivity is desired, the scope probe should be shifted to TP2.

C. Null Detector

These instructions should be followed by reference to Fig. 6.
CAUTION: Cover plate must be on to prevent oscillation.

1. Monitor TP2. Adjust L_1, L_2, and L_3 for maximum output. If the voltage at TP2 is greater than 1 volt, pp, the bridge should be adjusted for a better null.

2. Monitor TP3, depress SW1, then adjust L_4, L_5, and C_d for maximum output. NOTE: Before assembly, the L_6 slug is positioned so that the inductance from the tap to each end of the coils is the same. (Use LC meter.)

3. The phase-sensitive detector is normally operated so that the reference and signal voltages are either in or out of phase, depending upon the direction of bridge unbalance. This relationship can be verified with a dual-trace oscilloscope, externally synchronized from Ref and set for "alternate sweep." This is done as follows:

   a. Monitor TP5 with one scope probe, depress SW1, then adjust L_7 and L_8 for maximum.

   b. Monitor TP3 with the other scope probe, depress SW1, then adjust L_8 for the proper phase relationship. The waveforms at TP3 and TP5 should be either in or out of phase, depending upon the direction of bridge unbalance.

D. Zero, Gain, and V_0 Controls

Refer to Fig. 6. The bridge has been adjusted for null with each of the above controls in its maximum counterclockwise position. This is equivalent to open-loop operation with V_0 at zero volts. As manometer sensitivity is proportional to V_0, we normally operate with a V_0 appropriate to the pressure under measurement. We also operate closed-loop in order to improve linearity and to minimize the effects of membrane properties and changes in gain. With this in mind, we adjust the above controls as follows:

1. Set V_0 to a value suitable to the measurement. This is a function of manometer properties, and is treated mathematically by Cope.[4] A typical calibration is furnished by Opstelten and Warmoltz.[5]

2. Advance the gain control clockwise approximately one-fourth turn.

3. Monitor TP2 with a test probe, then adjust the zero control for null.

4. If additional loop gain is desired, the gain control may be advanced even further, and the zero control modified accordingly. If oscillations become evident, the gain and zero controls must be retarded. (A phase-correcting network will be added when the manometer design is complete, and oscillation should not be a problem.)

VI. FUTURE CONSIDERATIONS

As indicated earlier, the membrane manometer must be replaced with a more stable unit. One alternative is a pressure sensor manufactured by the Decker Corporation of Bala Cynwyd, Pennsylvania. The capacitance of their unit is about 10 pF, so it must be shunted with an external capacitor to bring the total to approximately 75 pF. This, of course, reduces sensitivity, but it may prove more expedient to use this than to manufacture a manometer with the desired properties. Also important, their manometer could be enclosed by a chamber wherein the temperature is held to close tolerances.

Concerning the generator, the differential capacitor C_g is to be shunted with a vernier capacitor of 0.5 to 5 pF. This will facilitate the null adjustment.

As manometer sensitivity influences the loop gain, it is desirable that the relevant properties be measured. The important measurements are capacitance change with pressure, electrostatic and mechanical.

With regard to nulling, the detection system is highly sensitive and so is susceptible to saturation. This indicates the need for precision nulling. If this becomes a problem it may prove practical to trade electronic gain for mechanical sensitivity at the diaphragm proper.

If additional gain is necessary to drive a low-impedance recorder, a difference amplifier should be inserted between the phase-detector output and recorder input.

ACKNOWLEDGMENTS

This work was sponsored by the Department of Chemical Engineering under the direction of Professor D. N. Hanson and performed under the auspices of the U. S. Atomic Energy Commission. The system was developed in collaboration with Peter Rony, who is to continue with the development and report on total performance. Part II of this report is by Mr. Rony[6] and describes micromanometer design and system performance.

APPENDICES

A. Null-Detector Gain Measurements

1. V1-gain of 37
   a. Input at pin 4 = 1 volt pp — 531 Scope, CA plug-in and (7 pF × 10 probe)
   b. Output at TP1 = 37 volt pp — (L_3 adjusted for maximum)

2. V2-gain of 32
   a. Input at TP1 = 1 volt pp
   b. Output at TP2 = 32 volts pp — (L_4 adjusted for maximum)

3. V3-gain of 35
   a. Input at TP2 = 1 volt pp
   b. Output at TP3 = 35 volts pp — (L_5 and C_d adjusted for maximum) (SW1 depressed and L_6 balanced)

4. Input transformer, L_1-L_2
   a. Input across L_1=0.22 volt pp — (L_1 adjusted for minimum)
   b. Output at pin 4 of V1 = 1.55 volts pp — (L_2 adjusted for maximum)
   c. Measured gain is 7 when driven from a zero-impedance source.
   d. Input impedance when tuned is approximately 10 ohms.
   e. Coupled impedance (reflected from secondary) is approximately 3 ohms.
   f. Gain when driven from bridge is approximately 3.
   g. ac resistance of each coil is approximately 6 ohms.
   h. Mutual inductance is approximately 3 μH.
   i. Coefficient of coupling is approximately 0.06.

5. Total gain of I through IV is 124,000

6. Detector gain
   a. If detector charges to peak value, the dc output voltage will be 1.4 times the rms input; this gives a gain of 1.4.

7. Total gain of I through V is 175,000 = dc output/rms input

8. Reference amplifier, V4. Total gain = 82, V4 gain = 54.
   a. Ref input 0.5 volt pp
   b. Output at plate of V4 = 27 volts pp — (L_7 tuned for maximum, SW1 depressed)
   c. Output at L_8 = 41 volts pp — (L_7 and L_8 tuned for maximum, SW_1 depressed)

B. Generator Voltage and Current Measurements

1. Current measurements
   a. Total plate current 11.5 mA
   b. Oscillator plate current 0.25 mA
   c. Buffer plate current 11.25 mA

2. Radio-frequency voltage measurements: 531 scope, CA plug-in and (7 pF × 10 probe)
   a. Maximum possible voltage at plate of V1 = 27 volts pp
   b. Maximum possible voltage at grid of V2 = 0.9 volt pp, 1.35 volts pp if V2 removed.
   c. Maximum possible voltage at plate of V2 if B_1 and B_2 connected to ground = 8.8 volts pp.
   d. Maximum possible voltage at Ref with B_1 and B_2 grounded = 0.8V pp.
   e. Maximum possible voltage at Ref when bridge connected and adjusted properly = 0.6V pp.

C. Coil Measurements

1. 25 turns, No. 22 Formvar, National Radio XR50 form
   a. Inductance range: 4.9 to 8.7 μH
   b. Q measurements
      (1) Q = 190 at 7.9 mc
          L = 5.45 μH
          C = 74.3 pF
      (2) Q = 144 at 3.14 mc
          L = 5.45 μH
          C = maximum at Q meter, over 450 pF
      (3) Q = 117 at 2.765 mc
          L = not measured
          C = maximum at Q meter, over 450 pF
      (4) Q = 111 at 2.765 mc
          L = not measured; resonates 450 pF to frequency
          C = 450 pF

2. 64 turns, No. 32 Formvar; National Radio XR50
   a. Inductance range: 30 to 56 μH
   b. Q measurements — Boonton Q meter, type 160A
      (1) Q = 131 at 2.5 mc
          L = 57.5 μH
          C = 70.7 pF
      (2) Q = 131 at 2.75 mc
          L = 57.5 μH
          C = 56.8 pF
      (3) Q = 155 at 2.765 mc — C set at 68 pF, L adjusted for resonance
          L = 59.5 μH
          C = 68 pF

(4) $Q = 152.5$ at 2.5 mc
$L = 48\ \mu H$
$C = 85$ pF

D. Null-Detector Transformer Measurements

Inductance was measured on two coils, each with 64 turns of No. 32 Formvar wire wound on National Radio form XR50; coils spaced 5/8 in. between centers. Inductance measurements were made with a Tektronix LC meter, type 130, and with coil slugs set at various positions. (M = mutual inductance; K = coefficient of coupling = $M/\sqrt{L_1 L_2}$; L_1 is inductance of the primary, L_2 inductance of the secondary.)

1. Both slugs fully out
   a. Measurements

   $L_1 = L_2 = 32.5\ \mu H$ (inductance, each coil)
   $L_1 + L_2 + 2M = 66.5\ \mu H$ (inductance, series-aiding)
   $L_1 + L_2 - 2M = 62\ \mu H$ (inductance, series-opposing)

   b. Conclusions

   $M = 1.125\ \mu H$
   $K = 0.0346$

2. a. Measurements

   $L_1 = L_2 = 34\ \mu H$ (inductance, each coil)
   $L_1 + L_2 + 2M = 72\ \mu H$ (inductance, series-aiding)
   $L_1 + L_2 - 2M = 66$ H (inductance, series-opposing)

   b. Conclusions

   $M = 1.5\ \mu H$
   $K = 0.044$

3. a. Measurements

   $L_1 = L_2 = 40\ \mu H$ (inductance, each coil)
   $L_1 + L_2 + 2M = 82\ \mu H$ (inductance, series-aiding)
   $L_1 + L_2 - 2M = 74\ \mu H$ (inductance, series-opposing)

   b. Conclusions

   $M = 2\ \mu H$
   $K = 0.05$

4. a. Measurements

   $L_1 = L_2 = 50\ \mu H$ (inductance, each coil)
   $L_1 + L_2 + 2M = 103\ \mu H$ (inductance, series-aiding)
   $L_1 + L_2 - 2M = 90\ \mu H$ (inductance, series-opposing)

   b. Conclusions

   $M = 3.25\ \mu H$
   $K = 0.065$

5. Both slugs fully in

   a. Measurements

      $L_1 = 58\ \mu H$, $L_2 = 60\ \mu H$ (inductance, each coil)

      $L_1 + L_2 + 2M = 125\ \mu H$ (inductance, series-aiding)

      $L_1 + L_2 - 2M = 105\ \mu H$ (inductance, series-opposing)

   b. Conclusions

      $M = 5\ \mu H$

      $K = 0.085$

REFERENCES

1. J. J. Opstelten, N. Warmoltz, and J. J. Zaalberg van Zelst, A Direct-Reading Double-Sided Micromanometer, Appl. Sci. Res. Sect. B6, 129 (1956).

2. J. J. Zaalberg van Zelst, Circuit for Condenser Microphones with Low Noise Level, Philips Tech. Rev. 9, 357 (1947).

3. The derivation, quite rigorous, is not presented here. If additional conditions are imposed as indicated, Eq. (3) results. Equation (3) is identical to that of another source. [See Eq. (18) of reference 4.]

4. J. O. Cope, Direct-Reading Diaphragm-Type Pressure Tranducers, Rev. Sci. Instr. 33, No. 9, 980 (1962).

5. J. J. Opstelten and N. Warmoltz, A Double-Sided Micromanometer, Appl. Sci. Res. Sect. B4, 329 (1955).

6. Peter R. Rony, The Design, Construction, and Operation of a Differential Micromanometer, Pt. II, Theory and Operational Characteristics, UCRL-11218 (in process).